Journal of King Saud University – Science 32 (2020) 486–495

Contents lists available at ScienceDirect

Journal of King Saud University – Science

journal homepage: www.sciencedirect.com

Original article

Numerical simulation of Rayleigh-Bénard convection in an inclined enclosure under the influence of magnetic field

M. Krishna Reddy *

Independent Researcher, Hyderabad, Telangana 500013, India

ARTICLE INFO

Article history:
Received 23 May 2018
Accepted 9 July 2018
Available online 10 July 2018

Keywords:
Convection
Finite element method
Heat transfer
Magnetohydrodynamics
Transient analysis

ABSTRACT

Two-dimensional numerical simulations are performed on the Rayleigh-Bénard convection using the finite element method, and the effect of the magnetic field on a thermally driven flow of a conducting fluid in a rectangular enclosure is studied. The simulations are performed on liquid Sodium with a Rayleigh number of 6×10^6 in a rectangular enclosure (aspect ratio – 4). The effects of the angle of declination of the enclosure and the influence of magnetic field in horizontal and vertical direction are examined. It is observed that the angle of declination of the enclosure (7°–28°) influenced the convection configurations with larger angles restraining the fluid velocity and hampering the formation of vortices. The applied magnetic field (0.001 T–0.003 T) too affected the formation of Bénard cells, and is dependent on the direction and the magnitude of the external field. In the presence of a horizontal magnetic field, a suppression of multiple vortices in favor of a singular cell structure is seen, and the degree of suppression is directly proportional to the magnitude of the field. Higher magnitudes of magnetic field suppressed convection with the isotherms showing lesser irregularities. However, vertical magnetic fields at smaller declination angles improved the circulation inside the enclosure leading to multiple well-defined parallel structures, which caused severe distortions in the temperature distributions. At large declination angles, the vertical magnetic field too suppressed the formation of well-defined Bénard cells.

1. Introduction

Thermal convection can be generalized as the heat transfer from one place to another by fluid movement. Free or natural convection takes places when the heat transfer occurs only due to the buoyancy forces that arise due to the density differences found in the fluid, which result from the temperature variations in the fluid. There has been an extensive study on natural convection over the years, and the Rayleigh-Bénard convection (Berge and Dubois, 1984; Lord Rayleigh, 1916; Tomita and Abe, 1999) has taken particular interest due to its simple mathematical formulation and the remarkable applications it has in the fields of science and engineering. In industrial applications, the Rayleigh- Bénard convection is seen in heat exchangers, crystal growth process and in cooling electrical components (Muthtamilselvan et al., 2018).

Two-dimensional numerical simulations performed by Ouertatani et al. (2008) demonstrated the influence of Rayleigh number on the pattern formation and temperature distribution. Chong et al. (2018) performed numerical simulations to study the effect of Prandtl number of the fluid and the geometry of the enclosure on natural convection. They stated that the aspect ratio and the Prandtl number of the fluid played a crucial role in pattern formation inside the enclosure. Muthtamilselvan and Sureshkumar (2017) also made similar observations regarding the effect of aspect ratio on natural convection.

Soong et al. (1996) investigated the effects of the inclination angle of an enclosure on the natural convection of fluid using numerical simulations. Multiple simulations with diverse Rayleigh numbers demonstrated that at higher inclination angles, multiple vortices are suppressed in favor of a singular cell structure. The "upslope and the downslope flow" at the walls of the enclosure governed the dynamics of the single-cell structure. Crunkleton and Anderson (2006) performed numerical simulations in a cubical enclosure at different inclination angles, which also demonstrated

* Address: Flat number 403, Dwaraka Residency, Sai Chitra Nagar, Ramanthapur, Hyderabad, Telangana 500013, India.
E-mail address: reddykrishna10596@yahoo.com
Peer review under responsibility of King Saud University.

Production and hosting by Elsevier

https://doi.org/10.1016/j.jksus.2018.07.010
1018-3647/

the effect of inclination angle on the fluid physics. Experiments on the free convection of liquid sodium in a long cylinder at different inclination angles performed by Kolesnichenko et al. (2015) also showed the dependence of inclination angle on heat transfer and fluid flow.

Along with the regular Rayleigh-Bénard convection, there has been a detailed study on the free convection in an electrically conducting fluid under the influence of a magnetic field (Arnou and Olsen, 2001; Chandrasekhar, 1961; Knobloch et al., 1981; Zierep, 2003). Magnetoconvection too has tremendous applications in the casting industry, solar technologies and in crystal growth of metals (Naffouti et al., 2014; Yu et al., 2018).

Libchaber et al. (1982) theorized that the free convection in the presence of an external magnetic field is driven by the contest between the flow steered by the temperature gradient and the counterflow guided by the Lorentz force. It is well established that the external magnetic field has a stabilizing effect on the convection flow (Arnou and Olsen, 2001; Burr and Müller, 2001; Nandukumar and Pal, 2015) and is found that the fluid flow is dependent on the direction and the magnitude of the applied field. With larger magnitudes, the magnetic field tends to orient the flow in the direction of the field. Tasaka et al. (2016) showed that the vertical magnetic fields affected the primary instability while the higher order instabilities are largely affected by the presence of a horizontal magnetic field.

An experiment performed by Burr and Müller (2001) investigated the Rayleigh-Bénard convection in liquid metal under the influence of vertical magnetic field and showed that the magnetic field damped the heat transport and significantly affected the convection patterns. Ece and Büyük (2006) performed numerical simulations on the natural convection under the influence of magnetic field in an enclosure heated and cooled on adjacent walls. They concluded that the convection flow inside the enclosure strongly depended on the aspect ratio, inclination angle, and the direction and magnitude of the magnetic field. Naffouti et al. (2014) studied the effects of the direction (different inclination angles) and the magnitude of magnetic field on convection by performing three-dimensional numerical simulations in a cubical enclosure. They too pointed out the dependence of the direction and magnitude of the magnetic field on the flow patterns and heat transfer. Selimli et al. (2015) studied numerically the combined effect of the electric and magnetic field on an enclosure containing liquid lithium. The results pointed out the dependence of direction and magnitude of the magnetic field on fluid physics. Further, the direction and magnitude of an electric field also altered fluid flow by increasing or decreasing the fluid velocity. Three-dimensional numerical simulations of Rayleigh-Bénard convection under the influence of magnetic field performed by Yu et al. (2018) demonstrated the effect of magnetic field on heat transfer and examined the evolution of Nusselt number with respect to the Hartmann number.

In the present study, two-dimensional simulations of the Rayleigh-Bénard convection are performed in a rectangular enclosure with a large aspect ratio using the finite element method. The variable parameters in the study are the angle of declination of the enclosure with the horizontal along with the direction and the magnitude of the magnetic field. The study outlines the influence of magnetic field and the angle of declination of the enclosure on the convection configuration and the temperature distribution.

It is shown that a small change in the declination angle altered the fluid physics and flow patterns. Larger declination angles decreased the stability of vortices leading to a decrease of the total number of vortices found inside the enclosure.

In the presence of a horizontal magnetic field, multiple vortices are suppressed in favor of a singular structure and higher declination angles hastened the process of suppression of vortices.

Concerning the vertical magnetic field, it is found that there is an increase in the number of Bénard cells at smaller declination angles. However, at higher declination angles, the vertical magnetic field too suppressed well-defined cells and affected the overall stability of the system.

2. Theory and mathematical formulation

Rayleigh-Bénard convection is a wonderful example of a self-organizing non-linear system and is a form of natural convection primarily governed by vertical temperature gradient and the influence of the gravitational force over the horizontal layer of the fluid. The fluid flow is symmetric and develops well-defined flow patterns known as Bénard cells (Ouertatani et al., 2008), and is analyzed by solving a set of Navier-Stokes equations and the heat equations simultaneously.

The Rayleigh number primarily governs the convention process (Muthtamilselvan et al., 2018). It is the product of the Grashof number and the Prandtl number and could be seen as a ratio of buoyancy and viscous forces (Sandberg et al., 2011). The Rayleigh number depends on the geometry on the enclosure, characteristic length and also on whether the top-surface is either free or closed.

$$Ra = GrPr = \frac{g\alpha\Delta TL^3}{\vartheta\kappa}$$

where ϑ is kinematic viscosity, α is the coefficient of thermal expansion, Tis the temperature, κ is the thermal diffusivity, and L is the characteristic length.

The Prandtl number of fluid mentioned in the above equation is the ratio of momentum diffusivity to thermal diffusivity. For fluids with very low Prandtl numbers, the thermal diffusivity dominates over the momentum diffusivity and plays a crucial role in the convection process (Chandra and Chhabra, 2012; Chong et al., 2018; Horanyi et al., 1999; Kolesnichenko et al., 2015).

With the flow primarily being driven by buoyancy, the Boussinesq approximations (Mihaljan, 1962) are assumed valid and are used in the Navier-Stokes equation. The approximation neglects the variation of density of the fluids in all terms excluding the gravitational term. The primary idea of the approximation is that there are no significant deviations of temperature and density from the mean value. The equations governing the Boussinesq approximation are represented below:

$$\nabla.u = 0$$

$$\frac{\partial u}{\partial t} + u.\nabla u = \frac{1}{\rho}\nabla p + \vartheta\nabla^2 u - g\alpha\Delta T$$

$$\frac{\partial T}{\partial t} + u.\nabla T = \kappa\nabla^2 T$$

In electrically conducting fluids, the convective flows are largely influenced by the presence of an external magnetic field. The magnetic field induces an electric current in a moving fluid, which causes a Lorentz force and in turn induces a magnetic field and alters the fluid flow. This type of flow is known as MHD flow.

To model an MHD flow, one must solve the Navier-Stokes equation and Maxwell's equations simultaneously. The dimensionless equations of MHD are (Gangl, 2016):

$$\frac{\partial B}{\partial t} = \nabla \times (u \times B) + \frac{1}{Re_m}\Delta B$$

$$\frac{\partial u}{\partial t} + (u.\nabla)u - \frac{1}{Re}\Delta u + \nabla p = NJ \times B$$

where Re is Reynold's number and $N = \sigma B^2 L/\rho V$ is the interaction term. $Re_m = VL\mu\sigma$ is the magnetic Reynold's number, which gives

an estimate of the relative effects of induction of magnetic field by fluid flow to the magnetic diffusivity. V is the characteristic velocity, $(\mu\sigma)^{-1}$ is the magnetic diffusivity and B is the magnetic field term.

In this study, the equations concerning convection using the Boussinesq approximation and the ideal MHD flow equations are solved at the same time.

3. Problem description and simulation

3.1. Description of the problem

A 2D rectangular enclosure is created and a geometrical representation of the problem with a declination angle of 7° is illustrated in Fig. 1. The length of the enclosure is L, while the height of the cavity is L/4 (aspect ratio – 4).

While performing the simulations, the declination angle of the enclosure is varied from 7° to 28° in the steps of 7°. The corner at the point A in Fig. 1 is taken as the pivot, and the declination angle with respect to the X-axis (angle XAB) is varied at this point.

Both the sides AB and CD are isothermal in nature, and a 1 K temperature difference is maintained between these sides of the enclosure. The other walls of the enclosure (sides BC and AD in Fig. 1) are considered to be adiabatic. The gravitational force is acting along the negative Y-axis.

Horizontal and vertical magnetic fields of magnitudes ranging from 0 T to 0.003 T are applied on the enclosure in all the four configurations to study the variation in the convection patterns seen in the fluid.

The fluid under the study is liquid sodium with a Rayleigh number of 6 x 10^6. The physical properties of the fluid are taken from the empirical relationships developed by Fink and Leibowitz (1995), and Sobolev (2010).

3.2. Simulation methodology

The geometry is drawn and meshed in Gmsh. A 2D unstructured mesh is generated using the "MeshAdapt" algorithm (Geuzaine and Remacle, 2009).

The simulation is performed in Elmer, which is an open source multiphysical simulation software mainly developed by CSC - IT Center for Science (CSC). Elmer employs Galerkin finite element approximation of weak for modeling the problem (Råback et al., 2017). A transient analysis is performed in the software where all the equations of fluid flow, heat transfer, and the MHD flow equations were coupled and solved simultaneously using the FlowSolve, HeatSolve and MagneticSolve modules (Råback et al., 2017).

The solutions to the equations used in the study are obtained via an iterative approach using Generalized Conjugate Residual algorithm (GCR), which is one of the Krylov subspace methods available in Elmer package (Ruokolainen et al., 2017). The convergence tolerance for all the solvers is set to 1.0×10^{-5}.

In the simulation, all the approximations of MHD and the Boussinesq approximations are taken into consideration with the absence of Joule heating as Joule heating is a second order term in the equation and has a negligible effect on the fluid flow (Vaux et al., 2015). A full-factorial design approach is employed (Pálfi and Geier, 2016) for the simulation to capture all the possible variations. The results are visualized in Elmer VTK and ParaView.

3.3. Model and solver validation

Simulations involving fluid flow (Safinowski et al., 2017), heat flow (Orlik-Kożdoń and Belok, 2017; Saldi and Wen, 2017) and MHD (Bondarenko et al., 2017) using Elmer have been studied in detail, and the capability of the solvers has been well established. Nevertheless, the accuracy of the solvers is checked by comparing the observations made using the software with the results found in the existing literature.

A simulation is performed on a fluid with Ra $\sim 10^6$ and Pr = 0.71 in a square enclosure. The Nusselt number is calculated at the hot wall to be 6.2257, which is in good agreement with the benchmark solutions proposed by Ouertatani et al. (2008), showing a deviation of 1.29%.

Further, 2D simulations are carried out in the presence of vertical magnetic field at Chandrasekhar numbers 670 and 1210, and Rayleigh numbers between 1.0×10^4 and 3.4×10^4 using liquid Gallium as the working fluid. Naffouti et al. (2014) showed that the 2D assumptions remain valid for simple 3D cases and hence, the results of the 2D simulation are compared with the experimental values. The Nusselt numbers obtained are in good agreement with the observations made by Aurnou and Olsen (2001).

4. Results and discussions

The term velocity ratio appearing in the subsequent discussion is the ratio of the velocity magnitude at a singular point on the axis to the maximum magnitude of the velocity observed across the entire reference axis of the enclosure. Peaks in the velocity ratio plots indicate higher magnitudes of the velocity of the fluid in that particular region, drawing to a conclusion that there was dominant flow perpendicular to the reference axis. The term 'Tm' in the subsequent discussion refers to the mean temperature of the enclosure. The term 'primary cell' refers to the first cell in the enclosure from the left in case of the presence of multiple vortices.

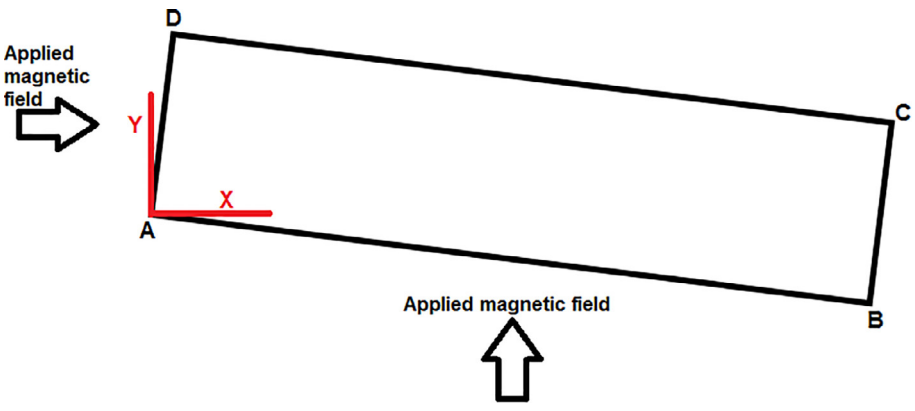

Fig. 1. Geometrical representation of the problem.

The glyphs representing the fluid flow in the discussion are scaled according to the velocity magnitude observed in that particular trial.

It is interesting to note that the flow maintained symmetricity in all the test cases.

4.1. Absence of magnetic field

The distribution of velocity ratio along the longer axis of the enclosure in the absence of a magnetic field at the end of the simulation time is plotted in Fig. 2.

The velocity magnitude of the fluid flow across the transverse axis of the enclosure showed a declining trend with an increase in the declination angle of the enclosure. Moreover, this effect was prominent in the latter half of the enclosure. The velocity ratio at the end of the enclosure (near side BC) dropped with an increase in the declination angle.

The stability found at the center of the vortices is reduced when the angle of declination is changed to 28°, and the same is evident in the plot, where the valleys throughout the graph ended at a higher value.

Visualizations in Fig. 3 better explain the drop in velocity ratios depicted in Fig. 2. The primary cell had a clockwise rotation and the subsequent cells showed anticlockwise and clockwise patterns in an alternating fashion.

At 7° declination, four well-defined cells with recirculating motion are observed. Along with these, two minor eddies are developed at the top of the enclosure. Increasing the declination angle to 14° also showed the development of four cells. However, eddies in the top of the enclosure seen are largely destroyed, and two new eddies are developed in the bottom half of the enclosure. At 21° declination, the boundary layer of the initial cell moved closer to the wall, while generating two eddies on top of each other at the bottom portion of the enclosure.

The last trail with 28° declination angle showed completely different behavior. Rather than the traditional four cells, only three-well defined cells are observed along with an elongated eddy at the bottom of the enclosure.

An increase in the declination angle moved the cells away from the right wall (BC) and closer to the left wall (AD). The void generated near the right wall is filled with irregular eddies. Moreover, in all the cases, the outer rims of the well-defined cells showed greater magnitudes of velocities compared to the outer rims of the irregular eddy.

The temperature distributions in the absence of a magnetic field are displayed in Fig. 4. At 7° declination, the first cell exhibited larger distortions, which are suppressed with an increase in the declination angle. Moreover, at higher declination angles, the latter half of the enclosure is dominated by temperatures well below the mean temperature, with the effect being more prominent in larger declination angles. The presence of irregular eddies and an increased downward fluid flow due to gravity at these locations caused the variation in temperature distributions. The temperature distribution plots of the well-defined cells observed in all the trials at the end of the simulation showed similarities with the observations made by Crunkleton and Anderson (2006), Ouertatani et al. (2008), and Soong et al. (1996).

4.2. Influence of horizontal magnetic field

The flow patterns are highly influenced by the introduction of a horizontal magnetic field. Fig. 5 shows the velocity ratio distribution present in the presence of a horizontal magnetic field. In all the cases, the boundary layer of the fluid flow is closer to the walls compared to what is seen in the absence of magnetic field.

The external magnetic field worked against the formation of the Bénard cells, and higher magnitudes of the magnetic field (0.002 T and 0.003 T) destroyed the multiple vortices in the enclosure that

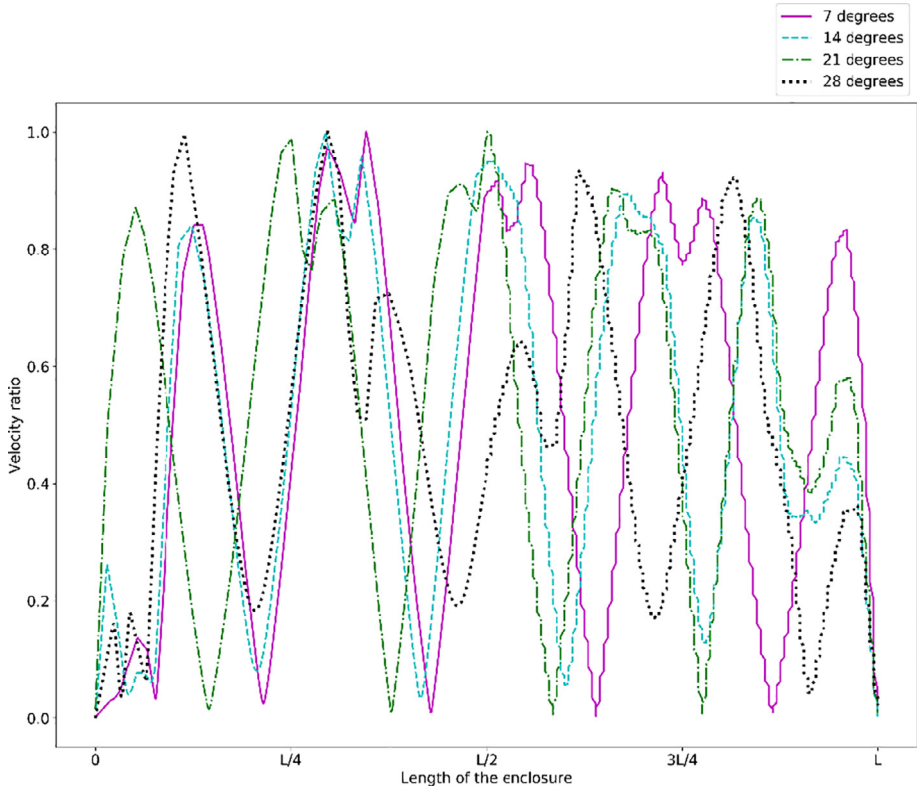

Fig. 2. Velocity ratio distribution in the absence of magnetic field.

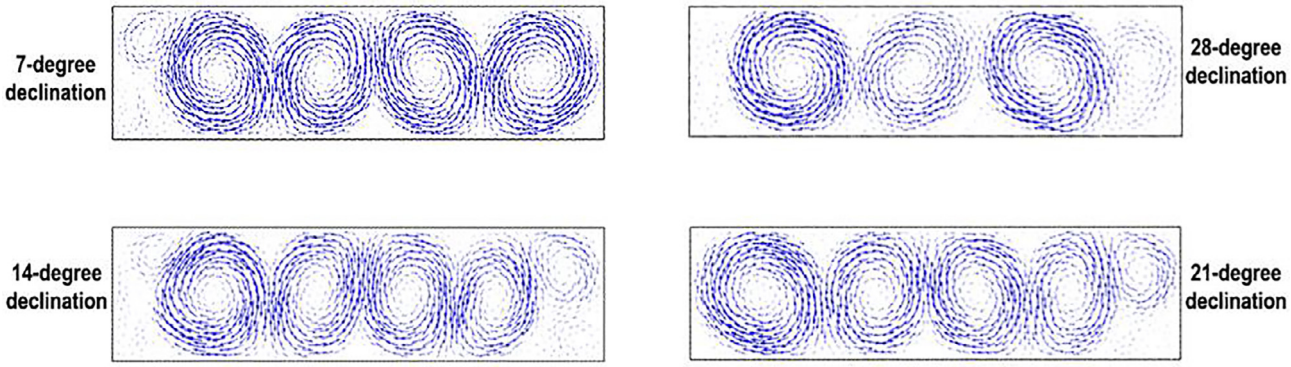

Fig. 3. Fluid flow in the absence of magnetic field.

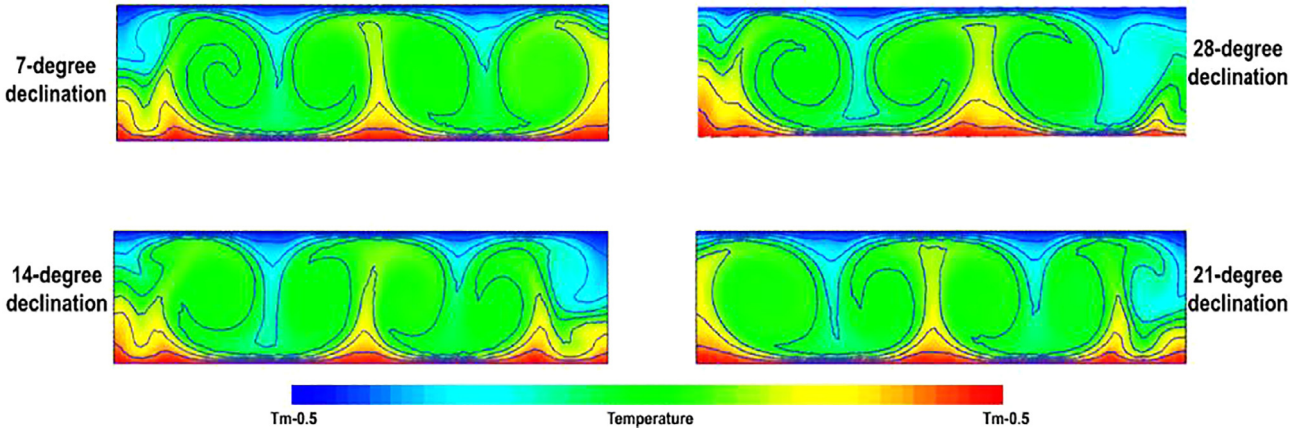

Fig. 4. Temperature contours in the absence of magnetic field.

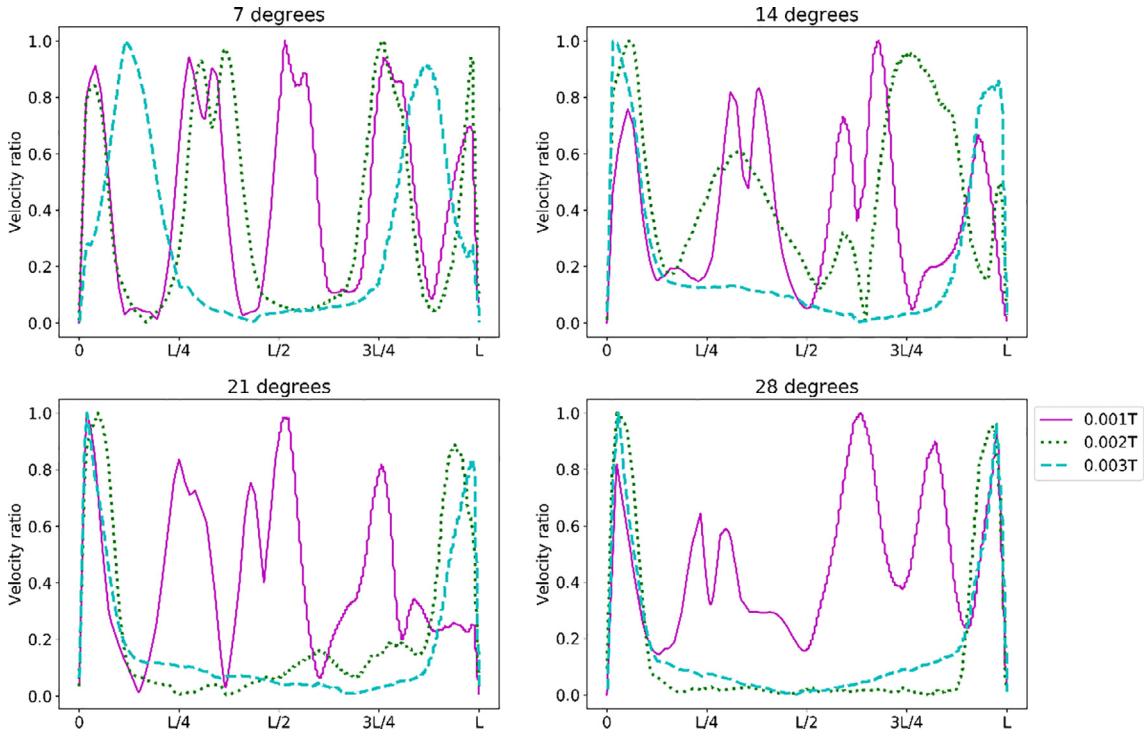

Fig. 5. Velocity ratio distributions in the presence of horizontal magnetic field.

are found in trials without a magnetic field (Fig. 3). Larger magnitudes of the magnetic field favored the formation of a single-cell flow over the formation of complex patterns.

The effect seen in this scenario is due to the stabilization effect of the horizontal magnetic field (Nandukumar and Pal, 2015). The stabilization effect happened due to MHD where the magnetic field acts on the fluid flow that is perpendicular to it, and the Lorentz force opposes the flow caused due to buoyancy forces. From Fig. 5, it is seen that at higher magnitudes, the influence of magnetic force becomes an important factor in determining the fluid physics.

Fig. 6 shows the convection patterns observed in the enclosure. An increase in the declination angle of the enclosure adversely affected the pattern formations in the presence of the horizontal magnetic field. Multiple vortices are present in the presence of weak magnetic field. At 7° declination, four cells are observed. As one moved towards larger declination angles, the Bénard cells decreased in number and showed elongations along the transverse axis of the enclosure. Elongated cells are observed at angles 14° and 21°. However, at 28° declination, three highly irregular eddies are observed indicating to the possibility that higher angles of declination would destroy multiple well-defined cells.

Larger magnitudes of magnetic field suppressed the vortices in favor of a singular-cell flow irrespective of the declination angle. The degree of suppression of multiple cells to a single-cell structure is directly proportional to the declination angle, which is observed by comparing the flow structures at 0.002 T across all configurations (Fig. 6).

In trials that exhibited multiple vortices, the primary cell showed a clockwise rotation. However, in one particular case at 7° declination, an increase in the magnitude of the magnetic field to 0.002 T showed flow reversal as described by Tasaka et al. (2016) with the primary cell exhibiting anti-clockwise rotation.

In all the cases that had a singular structure, the direction of the fluid flow is in the clockwise direction. The heated fluid ascended along the adiabatic wall at the higher end of the enclosure and then descended with a drop in temperature at the bottom half of the enclosure. This is captured in the isotherms presented in Fig. 7.

Fluctuations in the temperature distribution are severely damped in the presence of magnetic field (Ece and Büyük, 2006; Naffouti et al., 2014), and the effect is directly proportional to the magnitude of the magnetic field. The isotherms of the single-cell pattern showed similarities to the observations made by Soong et al. (1996). In trials that exhibited multiple irregular patterns (21° declination and 28° declination at 0.001 T), clear and prominent fluctuations of the temperature along the transverse axis of the enclosure are absent.

4.3. Influence of vertical magnetic field

Similar to what is seen in the presence of a horizontal magnetic field, the vertical magnetic field also influenced the flow patterns but in a drastically different way. Fig. 8 plots the velocity ratio distributions along the reference axis while Fig. 9 demonstrates the fluid flow in the enclosure.

Rather than suppressing the Bénard cells, the vertical magnetic field favored the formation of the vortices that showed clear parallel structures, and is in agreement with the observations made by Yu et al. (2018).

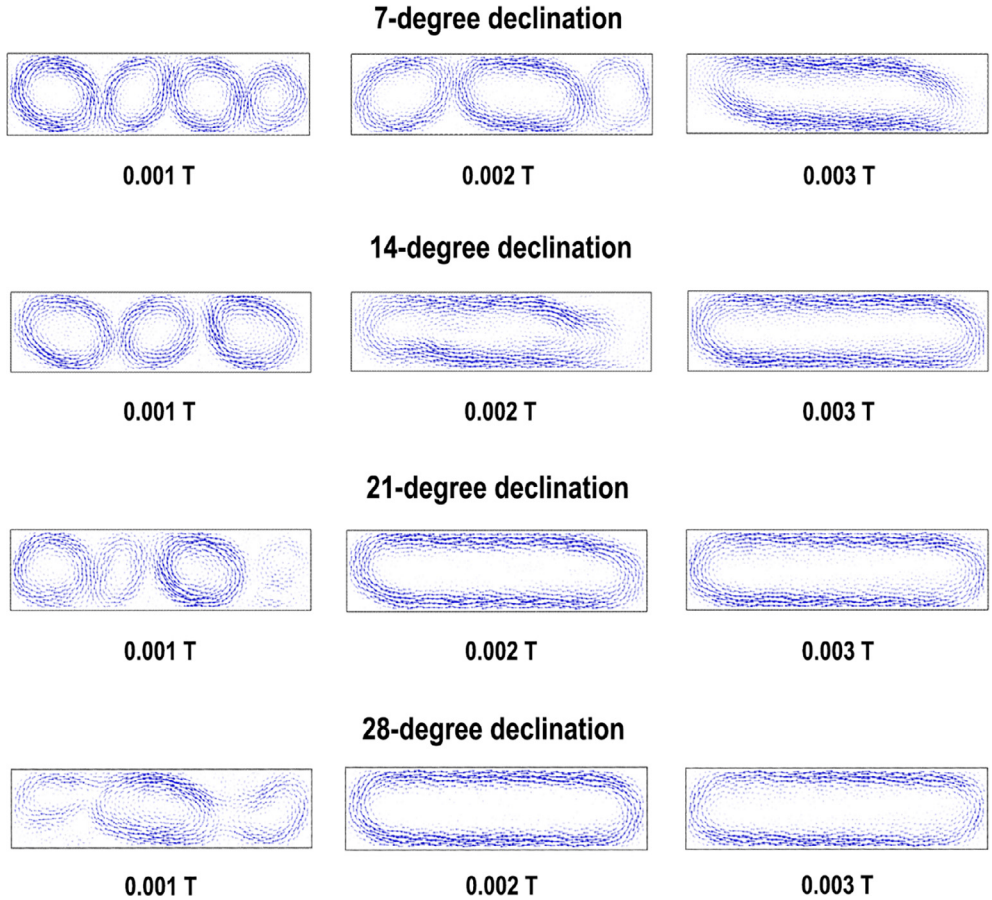

Fig. 6. Fluid flow in the presence of horizontal magnetic field.

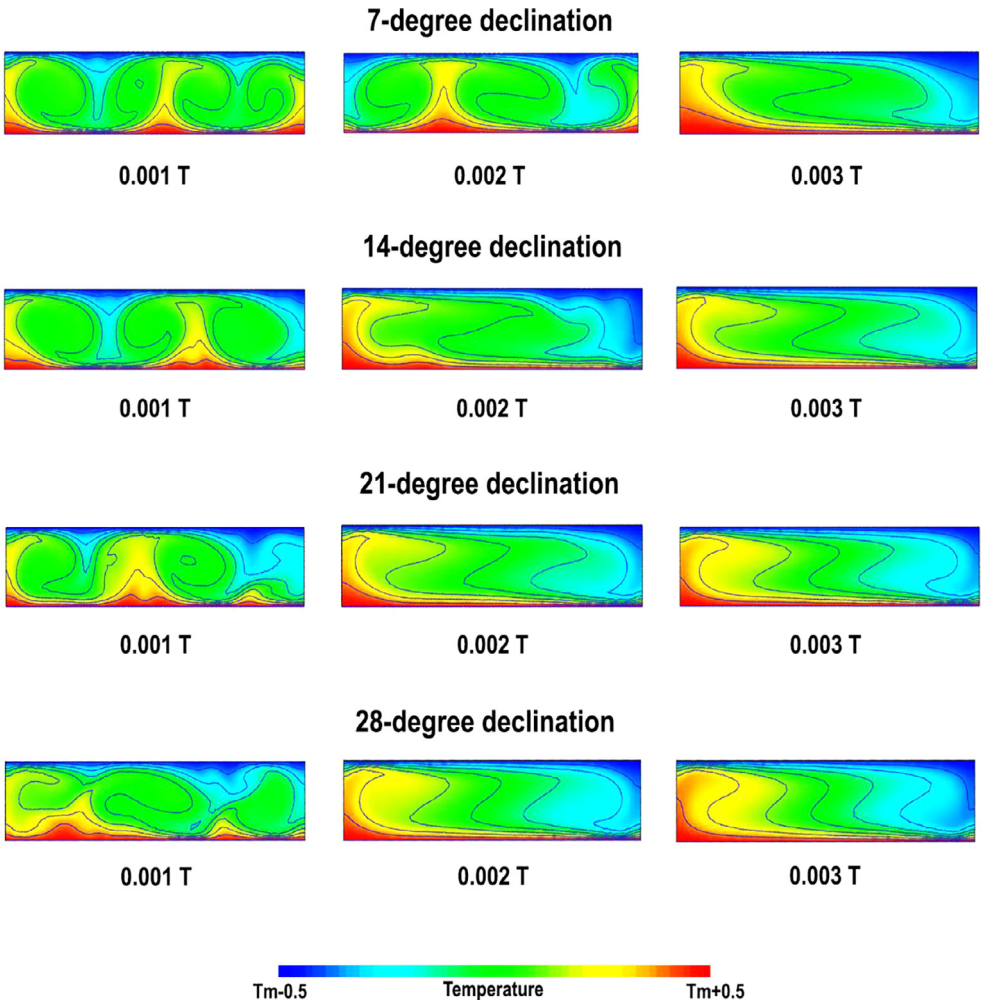

Fig. 7. Isotherms in the presence of horizontal magnetic field.

From Fig. 8, it is seen that the higher magnitudes of the vertical magnetic field suppressed the local velocity deviations seen in the outer rims of the Bénard cells giving rise to symmetrical peaks and valleys in the plot. Even at larger angles, the valleys in the plot ended at the same value of velocity ratio, which is caused due to the stabilization effect of the magnetic field. Furthermore, the mean transverse length of the vortices showed a reduction in magnitude as described by Burr and Müller (2001).

The primary cell in all the cases exhibited clockwise rotation. The subsequent cells in the enclosure exhibited anticlockwise rotation and clockwise rotation in an alternating fashion. At 7° and 14° declination, the presence of 0.001 T magnetic field caused the formation of three elongated eddies. An increase in the magnitude of the magnetic field led to the formation of five well-defined convection patterns. This number is greater than what is observed without a magnetic field (Fig. 3). This was due to the vertical magnetic field severely suppressing the horizontally aligned flow structures, which is in good agreement with the observations made by Naffouti et al. (2014).

At 0.001 T magnetic field, the 21° enclosure displayed four highly irregular eddies with one well-defined elongated cell at the middle. Increasing the magnetic field to 0.003 T made the flow more regular with five well-defined Bénard cells.

At 28° declination angle, the magnetic field distorted the vortices, which led to formation of two regular vortices and two irregular eddies in the presence of 0.001 T magnetic field. With 0.003 T magnetic field, the flow is disturbed further and the enclosure is void of the clear parallel structures seen in earlier observations. Two transversely elongated eddies along with one highly distorted eddy are observed.

Interestingly, a peculiar behavior is observed when the declination angle was higher than 14° and a 0.002 T magnetic field was applied. The top portion of the enclosure has well-defined convective flow patterns, while the bottom portion of the enclosure is completely void of it. The behavior in the latter part of the enclosure is similar to what was seen in the presence of a horizontal magnetic field. This could be due to the different equilibriums maintained by the buoyancy-driven flow with the magnetic field in the top and the bottom halves of the enclosure. This phenomenon is dependent on the magnitude of the magnetic field and no clear relationship could be established in this study, as a larger magnetic field did not exhibit this occurrence. Further simulations with different fluids and diverse Rayleigh numbers need to be conducted to further understand this phenomenon.

The temperature distributions are shown in Fig. 10. Several temperature distortions are observed in the presence of a vertical magnetic field with the regions with well-defined convection patterns showed larger distortions in temperature distributions. The distortions are much larger in the presence of a higher number of vortices in the enclosure.

The regions of extended vortices at 21° declination and 28° declination (0.002 T magnetic field) exhibited similar distributions

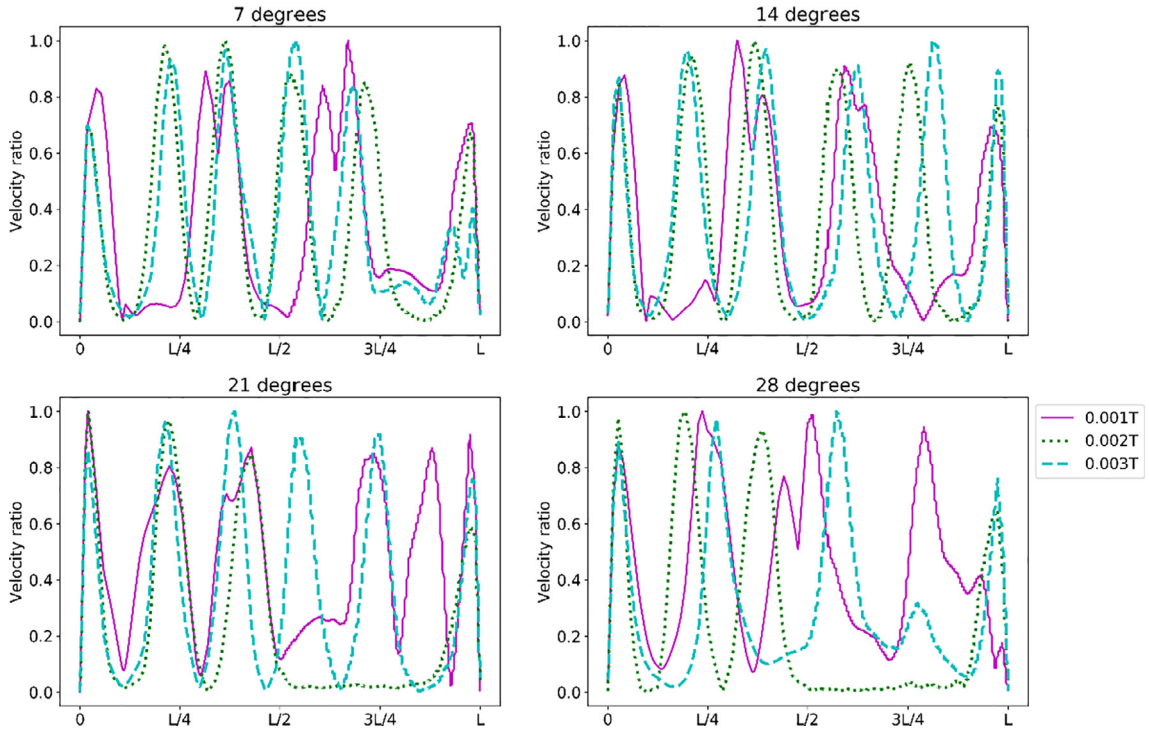

Fig. 8. Velocity ratio distribution in the presence of vertical magnetic field.

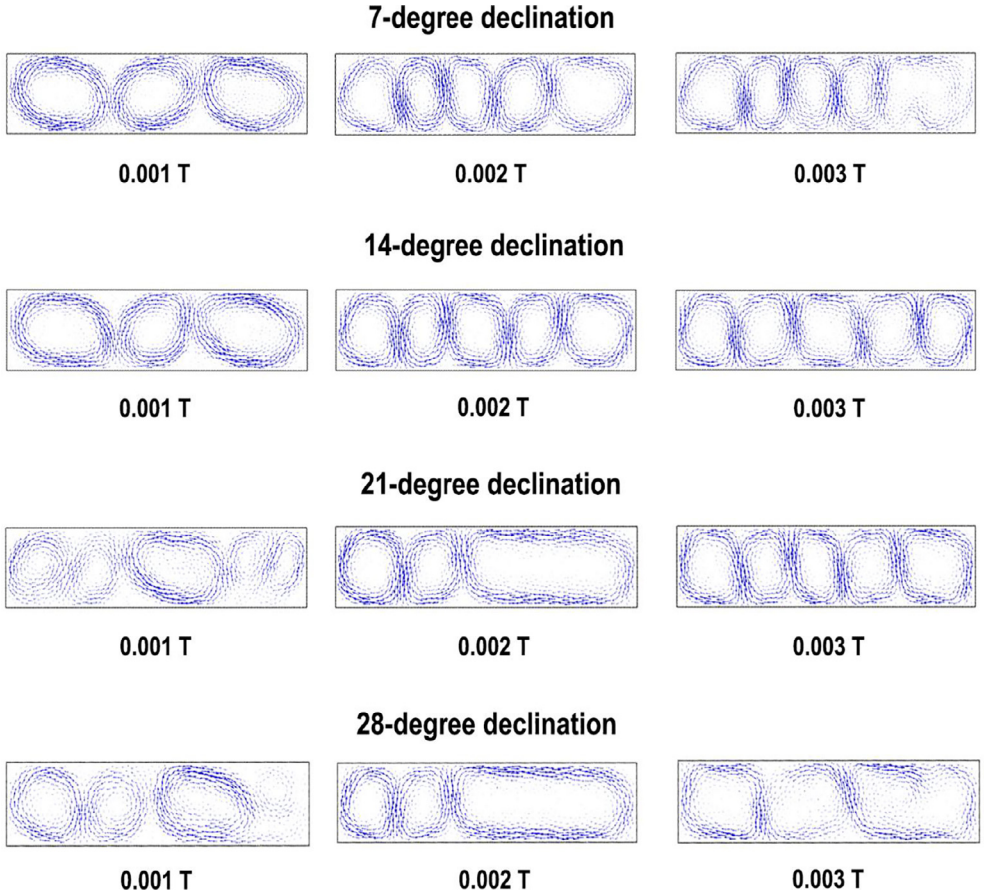

Fig. 9. Fluid flow in the presence of vertical magnetic field.

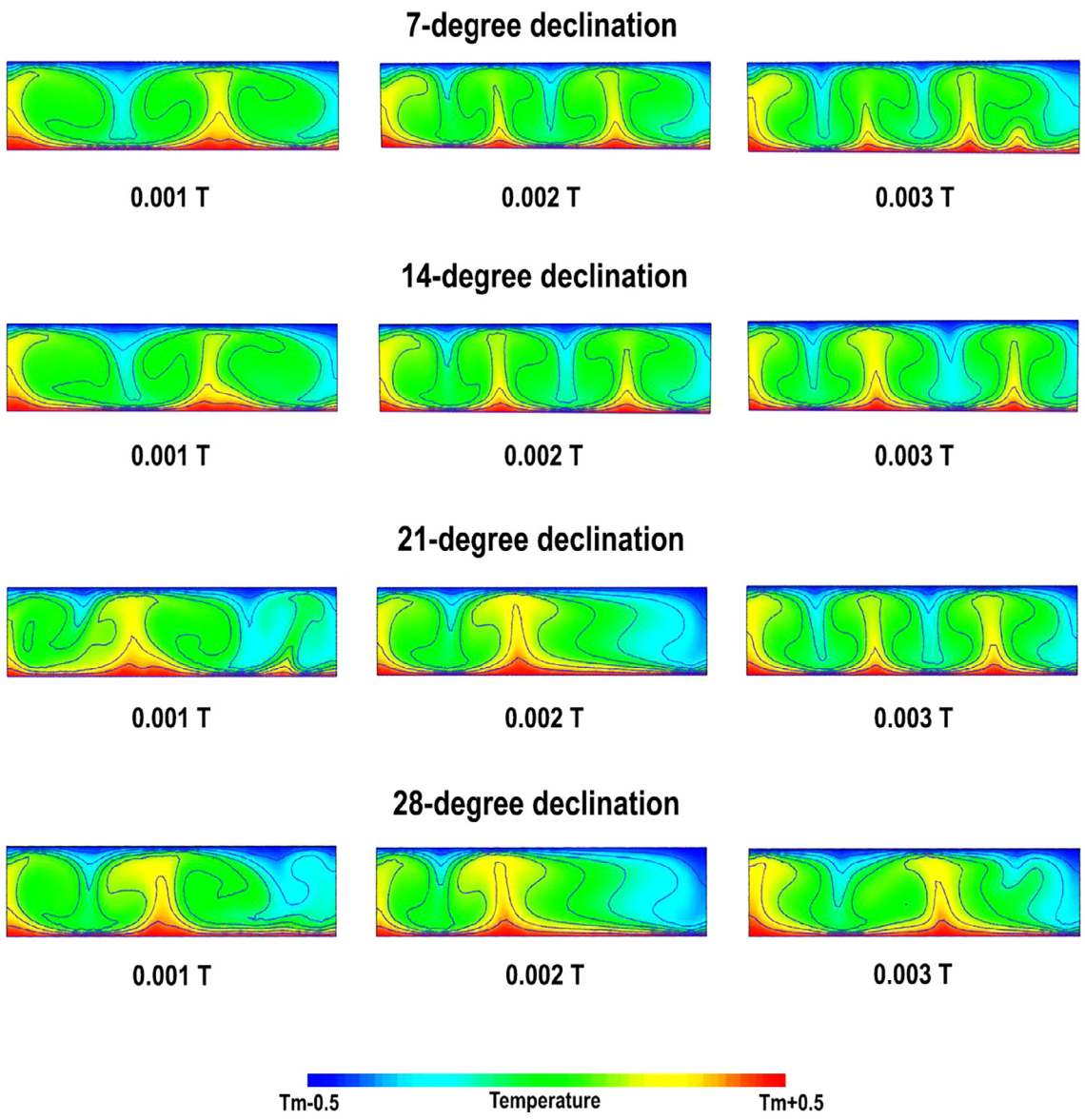

Fig. 10. Temperature distributions in the presence of vertical magnetic field.

of a singular cell seen in the presence of horizontal magnetic field. At 28° declination, the isotherms showed irregular patterns unlike any other, which is due to ill formation of well-defined vortices.

5. Conclusions

Two-dimensional simulations of Rayleigh-Bénard convection in an inclined enclosure under the influence of magnetic field is performed using the finite element method, and the following conclusions can be drawn:

1. In the absence of magnetic field, a four-cell pattern and a three-cell pattern with irregular eddies are observed. The simulations showed that the declination angle affected the pattern-formation inside the enclosure. The eddies present in the upper half of the enclosure vanished with the formation of irregular eddies in the lower half of the enclosure as one moved towards larger declination angles. The trend observed indicated that an increase in the angle of declination first destabilizes the well-defined vortices found the bottom half of the enclosure. Higher quantities of fluid flow due to gravity in enclosures with large declination angles is the primary driving force of this phenomenon.
2. The magnetic field in the horizontal direction suppressed the pattern formation. The magnetic field stabilized the fluid flow even at smaller declination angles. This effect is compounded with larger declination angles, which led to the formation of single symmetric cells due to the presence of a strong transverse flow. In addition, the temperature distributions showed smaller distortions in the presence of the horizontal magnetic field.
3. At small magnitudes, the Lorentz force due to the vertical magnetic field reduced the total number of vortices found in the enclosure. However, unlike the case of the horizontal magnetic field, higher magnitudes worked in favor of the formation of well-defined Bénard cells, which is seen at 7° and 14° declinations. Five well-defined cells are observed when the magnitude of the magnetic field was greater than 0.001 T.
4. At 28° declination, the vertical magnetic field suppressed pattern formation leading to the ill formation of well-defined cells indicating that the effect of gravitational force and the Lorentz force is greater than Buoyancy force. The temperature

distributions at this angle exhibited far fewer distortions compared to what is seen for angles below 28°.

5. Looking at the trend found in the observations of this study, a further increase in the declination angle of the enclosure would destroy multiple cells in favor of a single cell irrespective of the direction and magnitude of the magnetic field. Presence of a magnetic field would only hasten this process.

References

Aurnou, J., Olsen, P., 2001. Experiments on Rayleigh-Bénard convection, magnetoconvection and rotating magnetoconvection in liquid gallium. J. Fluid Mech. 430, 283–307.

Berge, P., Dubois, M., 1984. Rayleigh-bénard convection. Contemp. Phys. 25 (6), 535–582.

Bondarenko, D., Gabbar, A., C.A., H., Stoute, B., 2017. Engineering design of plasma generation devices using Elmer finite element simulation methods. Eng. Sci. Technol. Int. J. 20 (1), 160–167.

Burr, U., Müller, U., 2001. Rayleigh-Bénard convection in liquid metal layers under the influence of a vertical magnetic field. Phys. Fluids 13 (11), 3247–3257.

Chandra, A., Chhabra, R.P., 2012. Effect of Prandtl Number on Natural Convection Heat Transfer from a Heated Semi-Circular Cylinder. Int. J. Chem. Biol. Eng. 6, 69–75.

Chandrasekhar, S., 1961. Hydrodynamic and Hydromagnetic Stability. Oxford University Press, Clarendon Press, pp. 158–160.

Chong, K.L., Wagner, S., Kaczorowski, M., Shishkina, O., Xia, K.Q., 2018. Effect of Prandtl number on heat transport enhancement in Rayleigh-Bénard convection under geometrical confinement. Phys. Rev. Fluids 3, (1) 013501.

Crunkleton, W.D., Anderson, J.T., 2006. A numerical study of flow and thermal fields in tilted Rayleigh-Bénard convection. Int. Commun. Heat Mass Transf. 33, 24–29.

Ece, C.M., Büyük, E., 2006. Natural-convection flow under a magnetic field in an inclined rectangular enclosure heated and cooled on adjacent walls. Fluid Dyn. Res. 38, 564–590.

Fink, J.K., Leibowitz, L., 1995. Thermodynamic and Transport Properties of Sodium Liquid and Vapor. Reactor Engineering Division, Argonne National Laboratory, p. 1995.

Gangl, D.P., 2016. Introduction to Magnetohydrodynamics. Johannes Kepler Universität.

Geuzaine, C., Remacle, J.-F., 2009. Gmsh: a three-dimensional finite element mesh generator with built-in pre- and post-processing facilities. Int. J. Numer. Meth. Eng. 79 (11), 1309–1331.

Horanyi, S., Krebs, L., Müller, U., 1999. Turbulent Rayleigh-Bénard convection in low Prandtl-number fluids. Int. J. Heat Mass Transf. 42, 3983–4003.

Knobloch, E., Weiss, N., Costa, L., 1981. Oscillatory and steady convection in a magnetic field. J. Fluid Mech. 113, 153–186.

Kolesnichenko, I.V., Mamykin, A.D., Pavlinov, A.M., Pakholkov, V.V., Rogozhkin, S.A., Frick, P.G., Khalilov, R.R.I., Shepelev, S.F., 2015. Experimental study on free convection of sodium in a long cylinder. Therm. Eng. 62 (6), 414–422.

Libchaber, A., Laroche, C., Fauve, S., 1982. Period doubling cascade in mercury, a quantitative measurement. Journal de Physique Letters 43 (7), 211–216.

Rayleigh, Lord, 1916. On the convective currents in a horizontal layer of fluid when the higher temperature in on the under side. Philos. Mag. Ser. 6 (32), 529–546.

Mihaljan, J.M., 1962. A Rigorous Exposition of the Boussinesq Approximations Applicable to a Thin Layer of Fluid. Astrophys. J. 136, 1126–1133.

Muthtamilselvan, M., Sureshkumar, S., 2017. Convective heat transfer in a nanofluid-saturated porous cavity with the effects of various aspect ratios and thermal radiation. Phys. Chem. Liq. 55 (5), 617–636.

Muthtamilselvan, M., Periyadurai, K., Doh, H.D., 2018. Impact of nonuniform heated plate on double-diffusive natural convection of micropolar fluid in a square cavity with Soret and Dufour effects. Adv. Powder Technol. 29 (1), 66–77.

Naffouti, A., Ben-Beya, B., Lili, T., 2014. Three-dimensional Rayleigh-Bénard magnetoconvection: effect of the direction of the magnetic field on heat transfer and flow patterns. Comptes Rendus Mécanique 342 (12), 714–725.

Nandukumar, Y., Pal, P., 2015. Oscillatory instability and routes to chaos in Rayleigh-Bénard convection: effect of external magnetic field. EPL 112 (2).

Orlik-Kożdoń, B., Belok, J., 2017. Experimental and numerical study on the effective thermal conductivity of channel thermal insulation plate. Int. J. Heat Mass Transf. 106, 1097–1106.

Ouertatani, N., Cheikh, N.B., Beya, B.B., Lili, T., 2008. Numerical simulation of two-dimensional Rayleigh-Bénard convection in an enclosure. Comptes Rendus Mécanique 336, 465–470.

Pálfi, N., Geier, N., 2016. A comparative study of full factorial and central composite designs through the machining of aluminium alloy. Bánki.

Råback, P., Malinen, M., Ruokolainen, J., Pursula, A., Zwinger, T., Eds, 2017. Elmer Models Manual. CSC – IT Center for Science.

Ruokolainen, J., Malinen, M., Råback, P., Zwinger, T., Pursula, A., Byckling, M., 2017. Elmer Solver Manual. CSC – IT Center for Science.

Safinowski, M., Szudarek, M., Szewczyk, R., Winiarski, W., 2017. Capabilities of an Open-Source Software, Elmer FEM, in Finite Element Analysis of Fluid Flow. Recent Advances in Systems, Control and Information Technology.

Saldi, Z.S., Wen, J.X., 2017. Modeling thermal response of polymer composite hydrogen cylinders subjected to external fires. Int. J. Hydrogen Energy 42 (11), 7513–7520.

Sandberg, M., Berg, N., Johnsson, G., 2011. Rayleigh-Bénard convection. Royal Institute of Technology.

Selimli, S., Recebli, Z., Arcaklioglu, E., 2015. Combined effects of magnetic and electrical field on the hydrodynamic and thermophysical parameters of magnetoviscous fluid flow. Int. J. Heat Mass Transf. 86, 426–432.

Sobolev, V., 2010. Database of thermophysical properties of liquid metal coolants for GEN-IV. The Belgian Nuclear Research Centre.

Soong, Y.C., Tzeng, Y.P., Chiang, C.D., Sheu, S.T., 1996. Numerical study on mode-transition of natural convection in differentially heated inclined enclosures. Int. J. Heat Mass Transf. 39 (14), 2869–2882.

Tasaka, Y., Igaki, K., Yanagisawa, T., Vogt, T., Zuerner, T., Eckert, S., 2016. Regular flow reversals in Rayleigh-Bénard convection in a horizontal magnetic field. Phys. Rev. E 93 (4).

Tomita, H., Abe, K., 1999. Numerical simulation of the Rayleigh-Bénard convection of air in a box of large aspect ratio. Phys. Fluids 11 (3), 743–745.

Vaux, S.R.d., Zamansky, R., Bergez, W., Tordjeman, P., Bouyer, V., Piluso, P., Haquet, J. F., 2015. Magnetic field effects on three-dimensional natural convection. 22nd Congrès Français de Mécanique, Lyon.

Yu, X., Zhang, J., Ni, M., 2018. Numerical simulation of the Rayleigh-Benard convection under the influence of magnetic fields. Int. J. Heat Mass Transf. 120, 1118–1131.

Zierep, J., 2003. Rayleigh-Bénard convection with magnetic field. Theoret. Appl. Mech. 30 (1), 29–40.